High-resolution electroluminescent imaging of pressure distribution using a piezoelectric nanowire LED array

Article *in* Nature Photonics · August 2013

DOI: 10.1038/nphoton.2013.191

CITATIONS
696

READS
1,569

8 authors, including:

Caofeng Pan
Chinese Academy of Sciences
323 PUBLICATIONS **29,329** CITATIONS
SEE PROFILE

Lin Dong
Zhengzhou University
181 PUBLICATIONS **10,746** CITATIONS
SEE PROFILE

Ruomeng Yu
Georgia Institute of Technology
54 PUBLICATIONS **7,610** CITATIONS
SEE PROFILE

nature photonics

ARTICLES

PUBLISHED ONLINE: 11 AUGUST 2013 | DOI: 10.1038/NPHOTON.2013.191

High-resolution electroluminescent imaging of pressure distribution using a piezoelectric nanowire LED array

Caofeng Pan[1,2], Lin Dong[1,2], Guang Zhu[1], Simiao Niu[1], Ruomeng Yu[1], Qing Yang[1], Ying Liu[1] and Zhong Lin Wang[1,2]*

Emulation of the sensation of touch through high-resolution electronic means could become important in future generations of robotics and human–machine interfaces. Here, we demonstrate that a nanowire light-emitting diode-based pressure sensor array can map two-dimensional distributions of strain with an unprecedented spatial resolution of 2.7 μm, corresponding to a pixel density of 6,350 dpi. Each pixel is composed of a single n-ZnO nanowire/p-GaN light-emitting diode, the emission intensity of which depends on the local strain owing to the piezo-phototronic effect. A pressure map can be created by reading out, in parallel, the electroluminescent signal from all of the pixels with a time resolution of 90 ms. The device may represent a major step towards the digital imaging of mechanical signals by optical means, with potential applications in artificial skin, touchpad technology, personalized signatures, bio-imaging and optical microelectromechanical systems.

Emulating human senses by electronic means has long been a grand challenge for artificial intelligence and is pivotal in the development of accessible and natural interfaces between man and machine[1,2]. In contrast to the senses of sight, hearing, smell and taste, touch remains stubbornly difficult to mimic, because emulating touching necessitates the development of high-spatial-resolution, high-sensitivity, fast-response and large-sized pressure sensor arrays. A few groups have demonstrated pressure sensor arrays that are made from assembled nanowires, organic transistors or microstructured rubber layers, and are based on a change in capacitance or resistance[3–7]. These have been applied to map strain distribution in a matrix format at a resolution on the order of millimetres. New approaches are therefore necessary to develop artificial skins that have a resolution better than 50 μm in order to come close to the performance of human skin[1].

Here, we report that a nanowire light-emitting diode (NW-LED)-based pressure sensor array can map the distribution of strain, pressure and force with an unprecedented resolution of 2.7 μm, which is about three orders of magnitude higher than that demonstrated in the literature and far exceeds the resolution defined by human skin. Each pixel comprises an n-ZnO nanowire/p-GaN LED that is sensitive to local pressure, force and strain as a result of the piezo-phototronic effect. A pressure image is obtained by reading out the electroluminescent signal from all of the pixels in parallel at a time resolution of 90 ms. If integrated with on-chip optical communication technology, the information received from this self-emitting light strain sensor array can be quickly transmitted and rapidly processed by optical technology, potentially enabling the development of a highly intelligent human–machine interface[8].

Piezo-phototronic effect

In piezoelectric semiconductor nanowires composed of ZnO and GaN, for example, because of their non-centrally symmetric crystal structure[9], piezoelectric polarization charges can be created at the end of each nanowire by applying strain, pressure or force. The piezo-phototronic effect is to use the inner-crystal piezopotential as a 'gate' voltage to tune/control the charge separation, transport and/or recombination in optoelectronic processes[10–13]. This effect has been used to enhance the performance of photocells[14–16], the sensitivity of photodetectors[17–19] and the external efficiency of an LED[20,21]. In the present work, strain-controlled LED emission is used as an approach to fabricate a rapidly responding, optically based pixel array of strain sensors to directly 'image' the force/pressure distribution on the device at a resolution of only a few micrometres. The design principle makes use of the piezo-phototronic effect to tune the local light-emitting intensity of individual NW-LEDs[20]. The two-dimensional intensity distribution then becomes a map of the pressure distribution on the surface.

Device design

The device was based on a patterned array of n-ZnO nanowires grown on a p-GaN thin-film substrate, with the *c*-axis pointing upwards from the film (Fig. 1a)[22–25], thereby forming an array of pixelled light emitters. After infiltrating the inter-nanowire space with polymethylmethacrylate (PMMA), a transparent indium tin oxide (ITO) film was deposited on top of the nanowire array to form a common electrode, instead of the cross-bar electrodes used in touchpad technology. A convex-character pattern (for example, 'ABC') was fabricated using a negative photoresist SU-8 mould on a sapphire substrate. Using such an elastic SU-8 mould on sapphire enables a uniform distribution of pressure over an area corresponding to that of the 'ABC' characters. The ZnO nanowires in contact with the convex part of the SU-8 mould are compressed along their axial direction, leading to the generation of a negative piezopotential in their upper parts, while the uncompressed nanowires generate no piezopotential (Fig. 1b). Details of the experimental set-up and measurement system are provided in Supplementary Section SA.

[1]School of Materials Science and Engineering, Georgia Institute of Technology, Atlanta, Georgia 30332-0245, USA, [2]Beijing Institute of Nanoenergy and Nanosystems, Chinese Academy of Sciences, Beijing, 100083, China. *e-mail: zhong.wang@mse.gatech.edu

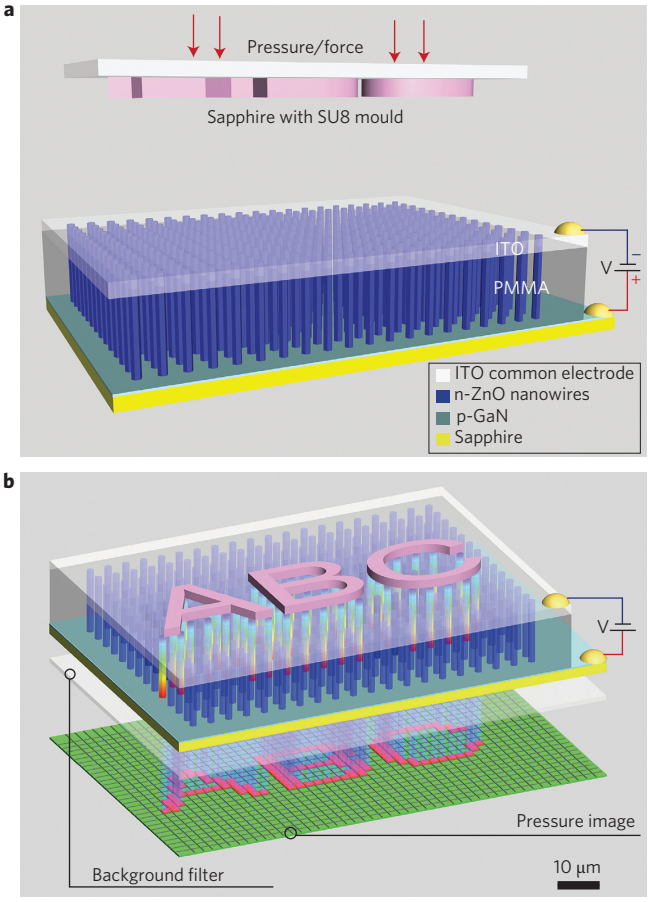

Figure 1 | Schematical device design and experimental approaches for imaging pressure distribution using the piezo-phototronic effect. a,**b**, Design of the NW-LED-based pressure sensor array before (**a**) and after (**b**) applying a compressive strain. The device is based on a patterned n-ZnO nanowire array, with the inter-nanowire space infiltrated with PMMA, and a transparent ITO layer as a common electrode. A convex character pattern, such as 'ABC', moulded on a sapphire substrate, is used to apply the pressure pattern on top of the ITO electrode. The ZnO nanowires that are covered by the mould are uniaxially compressed and a negative piezopotential is generated in their upper parts, as indicated by the colour code, while the nanowires untouched by the mould produce no piezopotential. For easy display of the internal structure of the device, the top sapphire substrate, on which the 'ABC' mould is mounted, is not shown in **b**.

We also carried out systematic finite element modelling (FEM) of device performance under external pressure, force and strain for different nanowire geometries (diameters and lengths), nanowire spacing, matrix modulus, and substrate thickness and modulus. The results established the robustness and stability of the device (Supplementary Section SB).

Working principle

Straining the basic unit cell of ZnO results in polarization of the cations and anions in the crystal because of its non-centrally symmetric structure, which is the root of the piezopotential inside the crystal. A schematic band diagram of a p-GaN/n-ZnO p–n junction composed of NW-LEDs, as shown in Fig. 2a, can be used to illustrate the piezopotential effect on the device before (black line) and after (red line) applying a strain. When the ZnO nanowire is under compressive strain, the strain inside the nanowire is much larger than that in the GaN film because of the low coverage of nanowires on the substrate surface (small contact cross-section), so a piezopotential is created in the nanowire. If the *c*-axis of the ZnO nanowires is pointing away from the GaN film[22–24], the presence of the non-mobile, positive ionic charges at the p–n junction region may result in a local dip in the band if the concentration of free carriers is low within the charge-depletion zone of the junction. The distorted band tends to temporarily trap holes near the GaN–ZnO interface, increasing the carrier injection rates towards the junction region, and increasing the recombination rate of electrons and holes. Furthermore, the presence of the piezopotential along the nanowire (Fig. 2b) is equivalent to applying an extra forward-biased voltage on the device. The depletion width and internal field are therefore reduced, and the injection current and emitting light intensity subsequently increased, when the device is compressed[10,26,27]. Our previous work demonstrated the enhancement of the light-emitting intensity (to ~400%) of a single-wire LED by straining using the piezo-phototronic effect[20]. The results are supported by a theory proposed for piezo-phototronics in relation to the photon emission at a p–n junction in the presence of local piezoelectric charges. In this theoretical work, analytical results under simplified conditions are presented with the aim of understanding the core physics of the piezo-phototronics devices, and numerical models are developed to illustrate the photon emission process and the carrier transport characteristics of a practical example of the piezoelectric LED[27]. Under forward bias, the light-emitting intensity of the nanowires under compressive strain is increased significantly, while the remaining nanowires under no strain show barely any change in electroluminescence intensity. Based on the intensity change of the emitting nano-LEDs, the pressure/strain distribution across the entire array can be mapped at a resolution of a few micrometres. This is the principle of our sensor array.

Results

The nanowires were fabricated by combining photolithography patterning and low-temperature wet chemical growth (Supplementary Section SC). Ordered arrays of vertical n-type ZnO nanowires were fabricated by uniform epitaxial growth on a p-GaN film to form the basic pixels of the sensors (Fig. 3a–c). Scanning electron microscopy (SEM) images clearly show that all the nanowires are wrapped by PMMA, and that the heads of the nanowires are exposed following oxygen plasma etching (Fig. 3d–f). A Ni/Au electrode was used to form ohmic contact with the bottom p-GaN, and an ITO layer was deposited in direct contact with the ZnO nanowires on top, thereby serving as common electrodes for the entire nanowire array (Fig. 3g,h). Notably, the position, diameter and length of the nanowire array could be well controlled experimentally with high precision and uniformity. Tiny fluctuations (for example, 1–2%) in the lengths of the nanowires would not affect the sensing result after depositing the top ITO electrode and packaging layer, because the large deformation arising from the ITO and packaging layer due to their low Young's moduli will tolerate small variations in nanowire length, as supported by FEM modelling (Supplementary Fig. S10, Section SB6).

The NW-LED array can be uniformly lit up under a bias of 5 V (Supplementary Section SD). An optical image of a lit LED array is shown in Fig. 4a, where each nanowire is a single light emitter and also a pixel unit. The centre-to-centre distance between two adjacent spots is 4 μm, corresponding to a pixel resolution of 6,350 dpi. Five typical NW-LEDs marked with a red rectangle in Fig. 4a are enlarged and displayed in Fig. 4b together with their intensity line profile. There is little crosstalk between adjacent pixels, and the actual resolution is 2.7 μm, as defined by the full-width at half-maximum (FWHM) of the emission pixels. The emission spectra obtained at different bias voltages (6, 7, 8, 9, 10 V) at room temperature are shown in Fig. 4c. Electroluminescence intensity increases with an increase in bias voltage, as expected from the band-bending

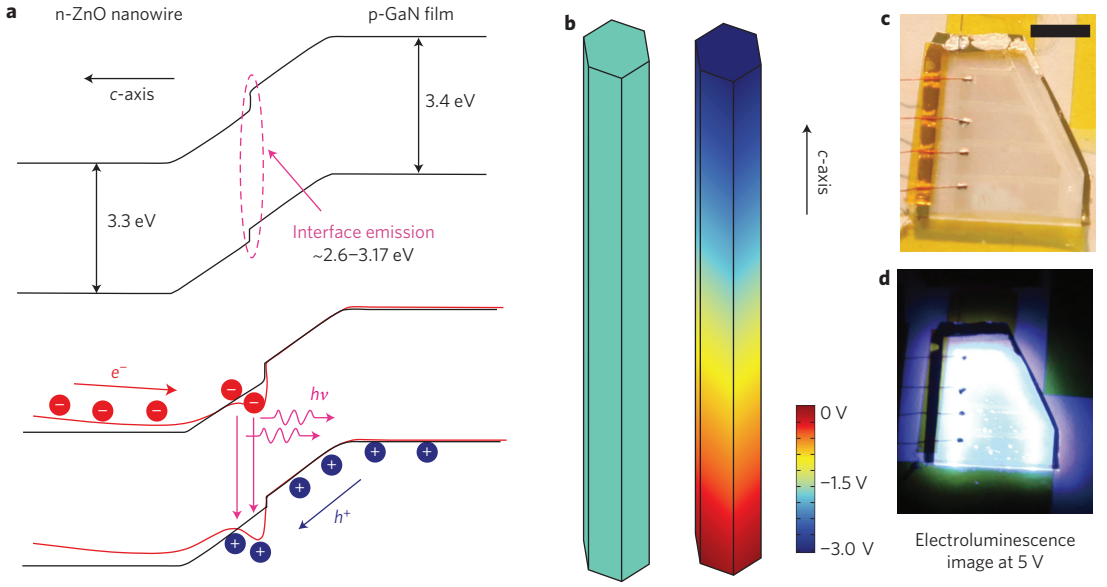

Figure 2 | Proposed mechanism for enhanced light emission in a NW-LED by the piezo-phototronic effect. a, Schematic band diagram of a p-GaN/n-ZnO p–n junction before (black line) and after (red line) applying a compressive strain, where the dip created at the interface is due to the non-mobile, positive ionic charges created by the piezopotential. **b**, Piezopotential distributions in a ZnO nanowire under −0.0186% strain simulated by a finite-element analysis method (COMSOL). The diameter and length used for calculation are 800 nm and 5 μm, respectively. The conductivity of the ZnO nanowire is ignored in the simulation for simplicity. **c**,**d**, Optical image of a fabricated device (**c**) and corresponding image when the device was electrically lit up at a bias voltage of 5 V, showing blue-white light emission from the NW-LED array (**d**). Scale bar in **c**, 5 mm.

model of a p–n junction[28]. The major emission peak located at 406 nm is identified as violet-blue emission, which can be associated with the interface emission[29] and does not show any obvious shift when the bias voltage is increased.

The NW-LED pressure sensor has a fast response and fast recovery. Figure 5a shows current versus time for five cycles of applied pressure. Response and relaxation times of less than 0.1 s were measured according to the enlarged plots in the inset to Fig. 5a; these were largely determined by the period of time needed to apply/retract the mechanical force. Indeed, the true response of our device is expected to be much faster than 0.1 s.

The emission intensity of a single-pixel NW-LED can be largely tuned/controlled by the magnitude of the applied strain. An image taken by a charge-coupled device (CCD) at zero applied strain is taken as the background signal, denoted I_o. An image of the LEDs taken under strain ε is denoted I_ε. The enhancement factor E of LED intensity is then defined as $E = (I_\varepsilon - I_o)/I_o$. Figure 5b shows factor E of a single representative NW-LED as a function of applied strain up to $\varepsilon = -0.15\%$. E is approximately linearly dependent on strain, and reaches 300% at a strain of −0.15%, in agreement with theoretical results[30] as long as the deformation of the ZnO nanowire is limited to the elastic range. The sensor sensitivity S in terms of relative light intensity enhancement as a function of applied pressure could be defined as[4]

$$S = \frac{\Delta I/I}{\sigma} = \frac{\Delta I/I}{140(\mathrm{GPa})|\varepsilon|} = \frac{1}{140}\frac{E}{|\varepsilon|}\mathrm{GPa}^{-1}$$

where E is the enhancement factor, σ the applied pressure, ε the strain in the ZnO nanowires, and we use 140 GPa as Young's modulus for the ZnO nanowires. For the device shown in Fig. 5b, $S \approx 12.88\ \mathrm{GPa}^{-1}$.

The stability and reproducibility of the NW-LED sensor array were studied by examining the light-emitting intensity of individual pixels when placed under −0.0186% strain for 25 on–off cycles of applied pressure. To exclude the crosstalk from adjacent pixels, a device consisting of sparsely distributed NW-LEDs was used for this investigation. Results for E of one NW-LED are shown in Fig. 5c (more results are presented in Supplementary Section SE). For this representative pixel, the average fluctuation of E was $\sim\pm5\%$, much smaller than the signal level. The high stability and repeatability demonstrated by the data demonstrate that the mechanical robustness of the NW-LEDs is sufficient for highly versatile pressure mapping. For the pixels we studied, the change in E shows no specific trend or synchronized pattern when the device is repeatedly compressed, indicating that the observed enhancement in light emission is dominated by the effect from piezoelectric charges at the ends of the nanowires rather than a change in contact area at the junction/interface, because a change in contact area would result in a synchronized change in E for all NW-LEDs during cycled mechanical straining (Supplementary Section SE1). The data presented in Fig. 6 further proves this conclusion. More experimental data, including repetitive on–off cycles of strain applied to a NW-LED array and the reversible step-by-step application of strain on a NW-LED array (consisting of over 20,000 NW-LED pixels), are provided in Supplementary Sections SE2 and SE3, and show very good repeatability and stability of our devices.

A two-dimensional mapping of strain was demonstrated using a convex character pattern of 'PIEZO' moulded on a sapphire substrate, which was directly applied onto the LED arrays as a seal (Fig. 6a). Figure 6b presents an optical image of the device with an SU-8 convex mould on top. Each black dot is a pixel comprising a single ZnO NW-LED with 4 μm pitch. Light-emitting images of the device at applied strains of 0, −0.06% and −0.15% were recorded by a CCD, as shown in Fig. 6c–e, respectively. The images unambiguously show that the change in LED intensity occurred at the pixels that were being compressed by the moulded pattern, while those not affected by the moulded characters showed almost no change in LED intensity. There was little crosstalk between adjacent pixels in the device.

The spatial strain distribution can be extracted from the LED intensity images. By carefully aligning the two images in Fig. 6c,e, an image for the enhancement factor $E(x,y) = [I_\varepsilon \quad (x,y)$

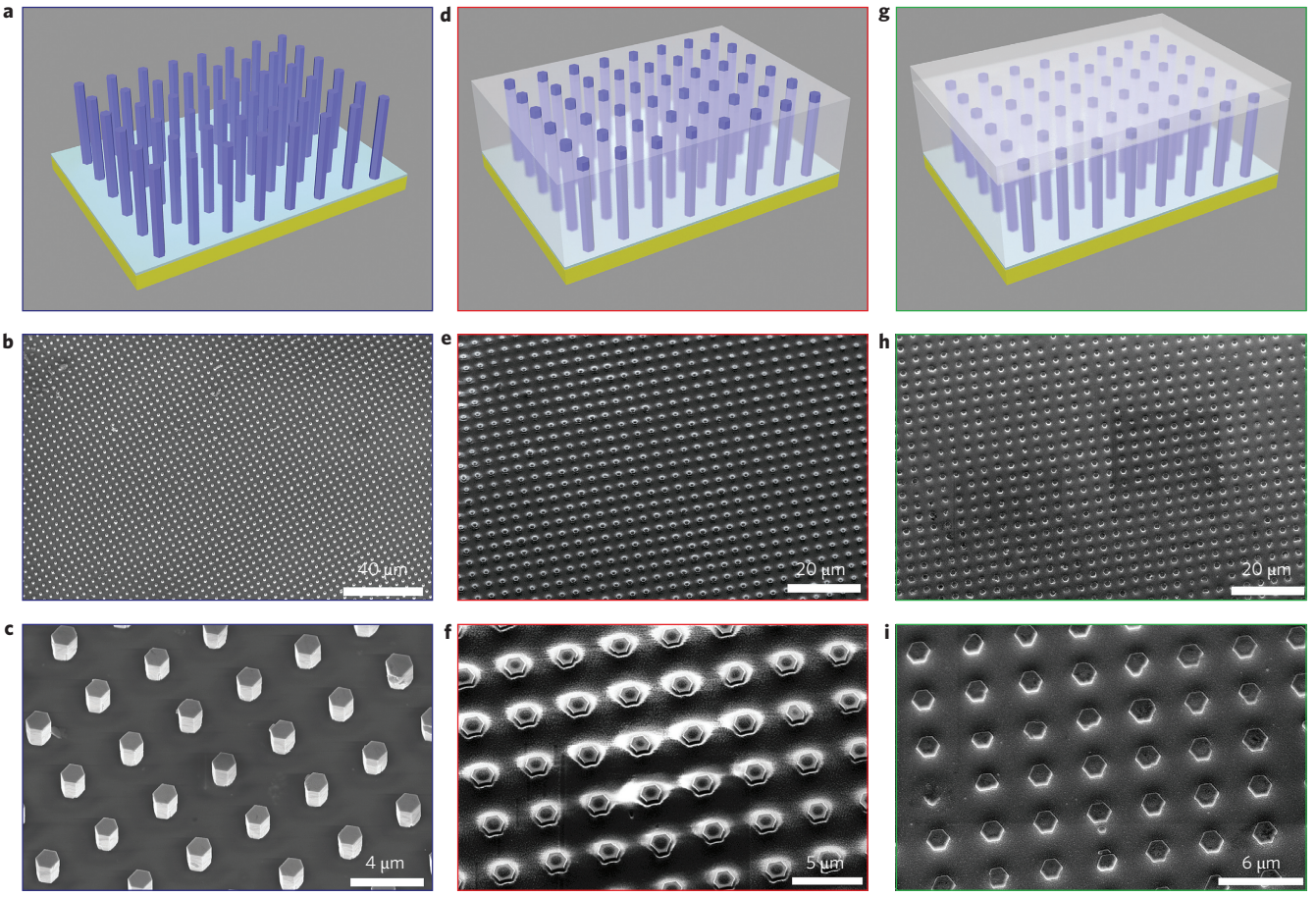

Figure 3 | Device fabrication. a, On a GaN/sapphire substrate, ZnO nanowire arrays are grown by combining photolithography patterning and low-temperature hydrothermal growth. **b**,**c**, SEM images of the as-grown ZnO nanowire arrays on the p-GaN film, with an average diameter of ~1.5 μm and pitch of 4 μm. **d**–**f**, A layer of PMMA is spin-coated to wrap around the nanowires. The fresh and clean tips of the nanowires are exposed after oxygen plasma etching, but the main body and bottoms of the nanowires are still fully enclosed, greatly improving the robustness of the structure. **g**–**i**, An ITO layer is deposited as a common electrode on top of the n-ZnO nanowires. Notably, both the Ni/Au electrode and the ITO electrode serve as common electrodes for the entire nanowire array for reading out in parallel the electroluminescent signal from all pixels.

$-I_o(x,y)]/I_o(x,y)$ was obtained, which is presented using a two-dimensional contour map in Fig. 6f, where (x,y) are the coordinates of the CCD pixels in the plane. The E image provides a spatial mapping of pressure applied to the entire array, and clearly shows the word 'PIEZO', originating from the mould. The colour code indicates that the average enhancement factor E is ~200%.

The signal-to-noise ratio of the E factor can be derived using the line profile data, as indicated for two positions in Fig. 6e—one on the moulded pattern (vertical pink line) and the other off the pattern (horizontal red line). The results are presented in Fig. 6g,h, respectively. The crosstalk is completely negligible, and the FWHM of the NW-LED pixels under strain is nearly the

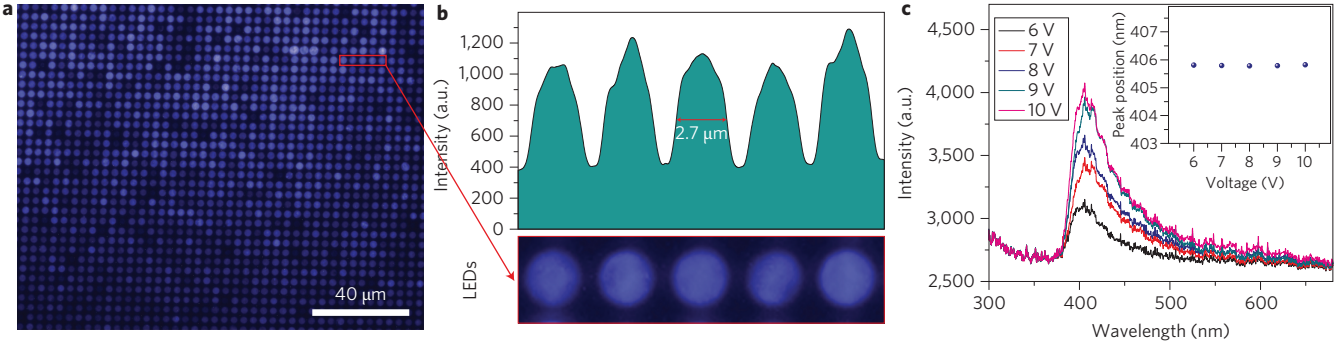

Figure 4 | Characterization of NW-LED arrays. a, Optical image of a NW-LED array when electrically emitting light. A nanowire is a single light emitter that also forms a pixel unit in the sensor array. **b**, Five typical nanowire LEDs (marked with a red rectangle in **a**) and a corresponding line profile of the emission intensity from which the possible spatial resolution achieved by the sensor can be estimated. **c**, Corresponding optical spectra of emitted light at bias voltages of 6, 7, 8, 9 and 10 V. Inset: dependence of peak position on applied voltage.

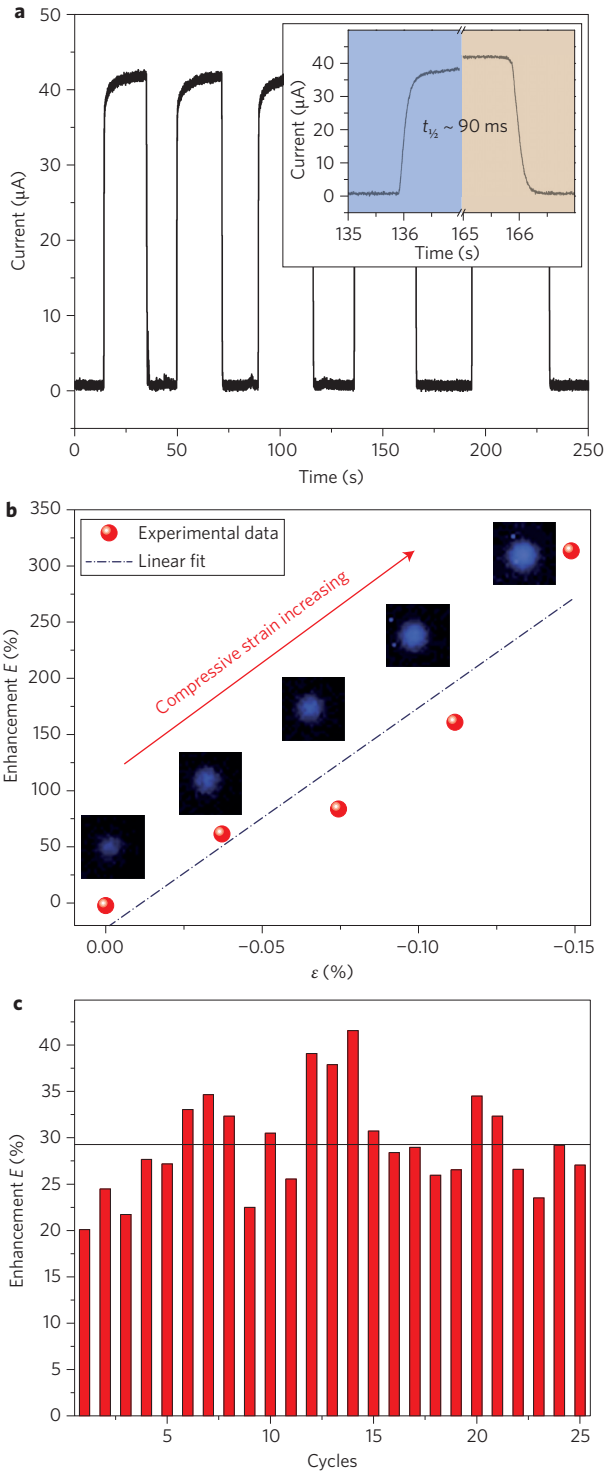

Figure 5 | Enhanced light emission of NW-LEDs under compressive strain by the piezo-phototronic effect. a, Fast response and recovery of the NW-LED pressure sensors. Inset: enlarged image of one cycle, showing response and recovery times of ~90 ms. **b**, Enhancement factor *E* of a NW-LED as a function of an applied compressive strain of up to $\varepsilon = -0.15\%$, together with the corresponding emitting light images. **c**, *E* factor of another nano-LED when repeatedly strained to −0.0186% strain for 25 on–off cycles, showing the good reproducibility of the LED intensity. The average fluctuation of the *E* factor in this device is ~5%, much smaller than the signal level (see **b**). This not only proves the stability and repeatability of the measurements, but also rules out the possibility of a change in contact area at the ZnO–GaN interface during mechanical straining.

same as in Fig. 4b, without strain. The *E* factor for the seven NW-LED pixels on the mould increased by a factor of 4–5 (up to 750%) when the applied strain increased from −0.06% to −0.15% (Fig. 6g). In contrast, the 36 NW-LED pixels that were off the mould pattern showed no enhancement at all, instead having a random variation at the noise level when the strain was increased from −0.06% to −0.15% (Fig. 6h). This unambiguously shows the gigantic effect of the piezoelectricity on LED emission. It proves the principle of using the piezo-phototronic effect for mapping pressure/strain at high spatial resolution, with high sensitivity and even high reliability. One further two-dimensional mapping of strain, with more than 20,000 LED pixels, is presented in Supplementary Section SF. This clearly illustrates the reproduction of the logo of Georgia Tech ('GT') by applying a compressive strain onto the device.

Discussion

The piezoelectric NW-LED-based approach offers a few unique advantages for imaging strain distribution. First, in contrast to other approaches such as cross-bar electrodes[3–5], where the pixels are the matrix defined by the electrodes so that the signal is measured and recorded in a sequential scanning mode, our pixels are defined by the distribution of nanowires on the substrate, all of which share two common electrodes (Fig. 1a). In this way, mapping is carried out simultaneously for all pixels at a time resolution of ~90 ms. Our parallel detection technology offers a much faster mapping rate for creating pressure distribution maps, and the time resolution is almost dictated by the relaxation process in applying/retracting the strain. Furthermore, our fabrication procedure could be simpler and cheaper than for the cross-bar electrode arrangement. Second, the spatial resolution is much higher and can be improved by optimizing the size and distribution of nanowires. The diameter of our nanowires was ~1.5 μm, as extracted from Fig. 3f, so the estimated resolution for our devices is given by $R(\mu m) = D + 1.2(\mu m)$, where $D(\mu m)$ is the diameter of the nanowires. If the diameter were reduced to 100 nm, we could obtain a resolution of 1.3 μm. Third, although our current study is based on a hard substrate, it is possible to extend the current approach to a soft substrate by directly cutting the current device into smaller units and then transferring these onto a soft substrate to follow a certain pattern[31]. Alternatively, we could fabricate ZnO p–n homojunction[32] arrays on any substrate (such as polydimethylsiloxane (PDMS)[33] or fibre[34]) (Supplementary Figs S18,S19, Section SG).

Finally, although there are some variations in the lighting intensity in different nanowires before strain is applied, possibly due to fluctuations in junction quality, such 'background' information can be removed using a signal-processing technique, such as defining an enhancement factor ($E = (I_\varepsilon - I_o)/I_o$) with a relative change of nanowire intensity before and after straining. Furthermore, growing high-quality nanowires using high-temperature vapour-phase techniques, such as metal–organic chemical vapour deposition (MOCVD), may also help to improve mapping quality.

Conclusions

In summary, we have presented the first nanowire LED-based pressure/strain sensor array that offers a spatial resolution of 2.7 μm for multipixel parallel mapping of strain, corresponding to a pixel density of 6,350 dpi, which is about three orders of magnitude higher than previously reported[3–5]. This approach is scientifically new because it relies on the piezo-phototronic effect for designing a stable, fast response, as well as parallel-detection strain-sensor arrays. The output signal is electroluminescence light, which is easy to integrate with photonic technologies for fast data transmission, processing and recording, and may enable the development of highly intelligent human–machine interfaces. This may represent a major step towards on-chip recording of mechanical signals by

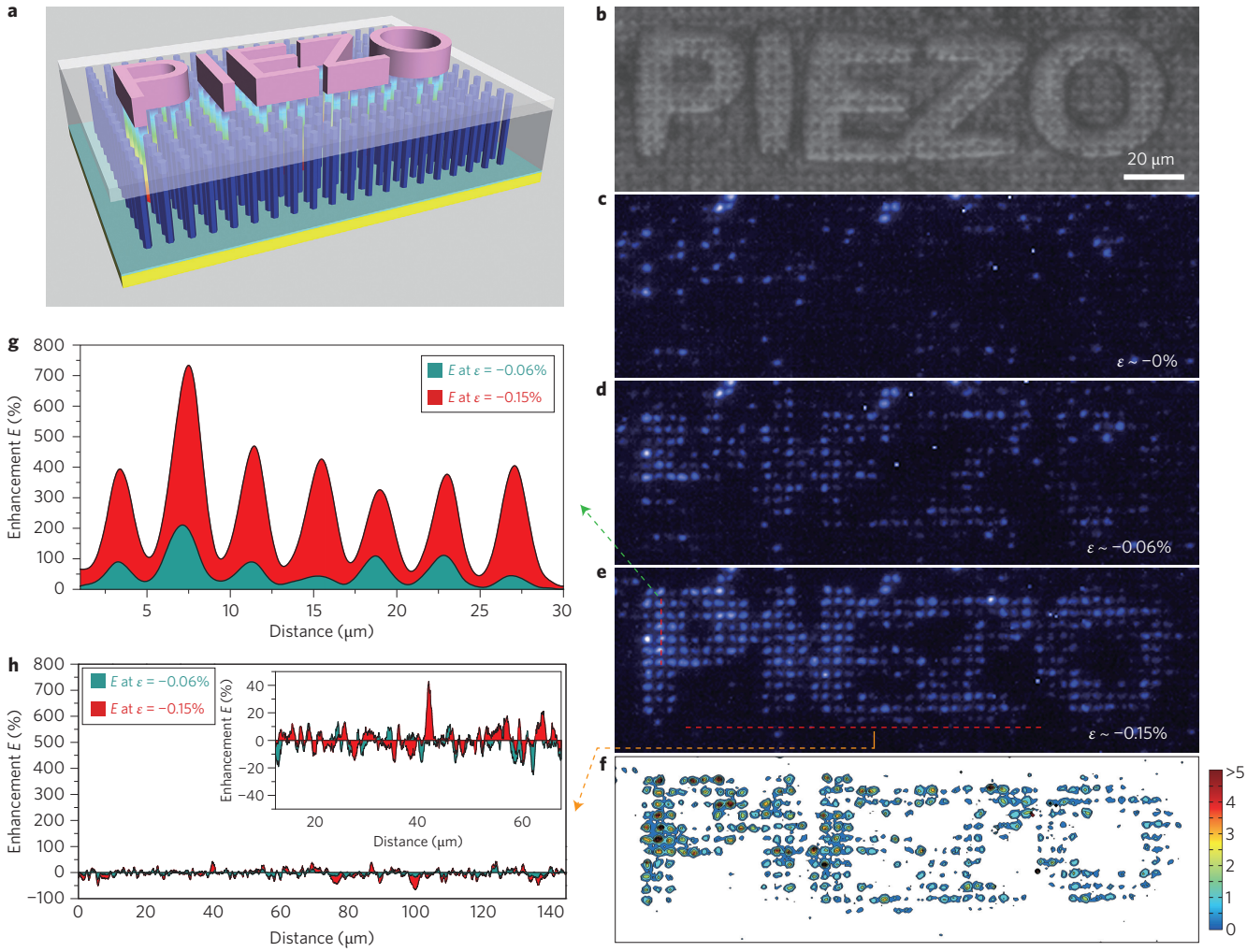

Figure 6 | High-resolution parallel imaging of pressure/force distribution. a, Illustration showing the working process of pressure distribution imaging. **b**, Optical image of the device with a convex mould on top. **c**–**e**, Electroluminescence images of the device at strains of 0, −0.06% and −0.15%, respectively. The images clearly show that a change in LED intensity occurred at the pixels that were compressed, while those away from the moulded pattern showed almost no change. **f**, Two-dimensional contour map of the $E(x,y)$ factor derived from the LED intensity images shown in **c** and **e**. It directly presents the word 'PIEZO', as given on the mould. **g**,**h**, Line profile data showing the signal-to-noise ratio of the E factor for two typical positions—one on the moulded pattern (vertical pink line, **g**) and one off the pattern (horizontal red line, **h**)—showing unambiguous differences.

optical means, with potential applications in touchpad technology, personalized signatures, bio-imaging and optical MEMS. Furthermore, with the feasibility of fabricating ZnO nanowires on flexible substrates, the current approach could be extended to smart skin with a resolution of ∼1.3 μm, which will have a great future in biological sciences, human–machine interfacing, smart sensor[35] and processor[36] systems, and even defence technology.

Methods

Patterned growth of ZnO nanowire arrays. A p-type 2 μm GaN film on *c*-plane sapphire fabricated by MOCVD was used. A 500-nm-thick SU-8 (Microchem) photoresist layer, with a patterned pore diameter of ∼800 nm and 4 μm pitch, was added by photolithography. The substrate with patterned SU-8 was then placed into a nutrient solution containing 15–50 mM zinc nitride (Alfa Aesar) and 15–50 mM hexamethylenetetramine (HMTA) (Fluka) to obtain nanowire growth at 95 °C for 3 h in an oven. Notably, the ZnO nanowires can be grown with a broad variation in nutrient solution concentration, from 5 mM to 100 mM. The concentration of the nutrient solution will control the growth speed, and nanowire length and diameter. The ZnO nanowires grew at the GaN sites exposed to the solution, and uniformly patterned ZnO nanowire arrays were accordingly obtained on a scale of centimetres.

Fabrication of devices. After growth of the ZnO nanowire arrays, 10 nm/100 nm layers of Ni/Au were deposited by electron beam evaporation onto the p-GaN, followed by rapid thermal annealing in air at 500 °C for 5 min. Subsequently, a relatively thick layer of PMMA (Microchem) was spin-coated to wrap around the nanowires. Oxygen plasma was then applied to etch away the top part of the PMMA, exposing the tips of the nanowires. Finally, a 100–300 nm ITO film was sputtered to form the top common electrode for the nanowires.

Imaging pressure distribution with a piezoelectric nano-LED array. The measurement system was built based on an inverted microscope (Nikon Ti-E), three-dimensional micromanipulation stages and a piezo nanopositioning stage (PI, P-753K078) with a closed-loop resolution 0.2 nm (Supplementary Section SA). A normal force/pressure was applied on the NW-LEDs using a sapphire substrate with a convex character pattern of 'PIEZO' moulded on it. By controlling the three-dimensional micromanipulation stages and the piezo nanopositioning stage, the pressure could be applied step by step with a fixed amount. A detailed calculation of the strain in the nanowires can be found in the Supplementary Information[20]. The output light intensity was recorded by a spectrometer (Master Systems Felix32 PTI) or CCD, which characterized the optical power in a relative manner. We mainly focused on the relative change in output light intensity under different strains. The data for investigating the influence of strain on light intensity and spectrum were recorded using a fibre-optical spectrometer. We monitored the pressure change from the change in light-emitting intensity using image acquisition and processing technologies.

Received 2 February 2013; accepted 26 June 2013; published online 11 August 2013

References

1. Boland, J. J. Flexible electronics within touch of artificial skin. *Nature Mater.* **9,** 790–792 (2010).
2. Kim, D. H. *et al.* Epidermal electronics. *Science* **333,** 838–843 (2011).
3. Mannsfeld, S. C. B. *et al.* Highly sensitive flexible pressure sensors with microstructured rubber dielectric layers. *Nature Mater.* **9,** 859–864 (2010).
4. Takei, K. *et al.* Nanowire active-matrix circuitry for low-voltage macroscale artificial skin. *Nature Mater.* **9,** 821–826 (2010).
5. Lipomi, D. J. *et al.* Skin-like pressure and strain sensors based on transparent elastic films of carbon nanotubes. *Nature Nanotech.* **6,** 788–792 (2011).
6. Someya, T. *et al.* A large-area, flexible pressure sensor matrix with organic field-effect transistors for artificial skin applications. *Proc. Natl Acad. Sci. USA* **101,** 9966–9970 (2004).
7. Zhu, J. J. *et al.* Effects of doping concentrations on the regeneration of Bragg gratings in hydrogen loaded optical fibers. *Opt. Commun.* **284,** 2808–2811 (2011).
8. Shambat, G. *et al.* Ultrafast direct modulation of a single-mode photonic crystal nanocavity light-emitting diode. *Nature Commun.* **2,** 539 (2011).
9. Wang, Z. L. & Song, J. H. Piezoelectric nanogenerators based on zinc oxide nanowire arrays. *Science* **312,** 242–246 (2006).
10. Wang, Z. L. Piezopotential gated nanowire devices: piezotronics and piezo-phototronics. *Nano Today* **5,** 540–552 (2010).
11. Wang, Z. L. Progress in piezotronics and piezo-phototronics. *Adv. Mater.* **24,** 4632–4646 (2012).
12. Wang, Z. L. *et al.* Lateral nanowire/nanobelt based nanogenerators, piezotronics and piezo-phototronics. *Mater. Sci. Eng. R* **70,** 320–329 (2010).
13. Wang, Z. L. *Piezotronics and Piezo-phototronics* (Springer, 2013).
14. Hu, Y. F. *et al.* Optimizing the power output of a ZnO photocell by piezopotential. *ACS Nano* **4,** 4220–4224 (2010).
15. Boxberg, F., Sondergaard, N. & Xu, H. Q. Photovoltaics with piezoelectric core–shell nanowires. *Nano Lett.* **10,** 1108–1112 (2010).
16. Pan, C. F. *et al.* Enhanced Cu_2S/CdS coaxial nanowire solar cells by piezo-phototronic effect. *Nano Lett.* **12,** 3302–3307 (2012).
17. Yang, Q. *et al.* Enhancing sensitivity of a single ZnO micro-/nanowire photodetector by piezo-phototronic effect. *ACS Nano* **4,** 6285–6291 (2010).
18. Gao, P. *et al.* Photoconducting response on bending of individual ZnO nanowires. *J. Mater. Chem.* **19,** 1002–1005 (2009).
19. Dong, L. *et al.* Piezo-phototronic effect of CdSe nanowires. *Adv. Mater.* **24,** 5470–5475 (2012).
20. Yang, Q., Wang, W. H., Xu, S. & Wang, Z. L. Enhancing light emission of ZnO microwire-based diodes by piezo-phototronic effect. *Nano Lett.* **11,** 4012–4017 (2011).
21. Yang, Q. *et al.* Largely enhanced efficiency in ZnO nanowire/p-polymer hybridized inorganic/organic ultraviolet light-emitting diode by piezo-phototronic effect. *Nano Lett.* **13,** 607–613 (2013).
22. Lee, S. H. *et al.* Ordered arrays of ZnO nanorods grown on periodically polarity-inverted surfaces. *Nano Lett.* **8,** 2419–2422 (2008).
23. Jasinski, J. *et al.* Application of channeling-enhanced electron energy-loss spectroscopy for polarity determination in ZnO nanopillars. *Appl. Phys. Lett.* **92,** 093104 (2008).
24. Bae, S. Y. *et al.* Synthesis of gallium nitride nanowires with uniform [001] growth direction. *J. Cryst. Growth* **258,** 296–301 (2003).
25. Xu, S. *et al.* Ordered nanowire array blue/near-UV light emitting diodes. *Adv. Mater.* **22,** 4749–4753 (2010).
26. Wang, Z. L. Piezotronic and piezophototronic effects. *J. Phys. Chem. Lett.* **1,** 1388–1393 (2010).
27. Zhang, Y. & Wang, Z. L. Theory of piezo-phototronics for light-emitting diodes. *Adv. Mater.* **24,** 4712–4718 (2012).
28. Lai, E., Kim, W. & Yang, P. D. Vertical nanowire array-based light emitting diodes. *Nano Res.* **1,** 123–128 (2008).
29. Hwang, D. K. *et al.* p-ZnO/n-GaN heterostructure ZnO light-emitting diodes. *Appl. Phys. Lett.* **86,** 222101 (2005).
30. Gao, Y. & Wang, Z. L. Electrostatic potential in a bent piezoelectric nanowire. The fundamental theory of nanogenerator and nanopiezotronics. *Nano Lett.* **7,** 2499–2505 (2007).
31. Xu, S. *et al.* Stretchable batteries with self-similar serpentine interconnects and integrated wireless recharging systems. *Nat. Commun.* **4,** 1543 (2013).
32. Yankovich, A. *et al.* Stable p-type conduction from sb-decorated head-to-head basal plane inversion domain boundaries in ZnO nanowires. *Nano Lett.* **12,** 1311–1316 (2012).
33. Zhang, S. *et al.* Growth and replication of ordered ZnO nanowire arrays on general flexible substrates. *J. Mater. Chem.* **20,** 10606–10610 (2010).
34. Pan, C. F. *et al.* Fiber-based hybrid nanogenerators for/as self-powered systems in biological liquid. *Angew. Chem. Int. Ed.* **50,** 11192–11196 (2011).
35. Patolsky, F. *et al.* Detection, stimulation, and inhibition of neuronal signals with high-density nanowire transistor arrays. *Science* **313,** 1100–1104 (2006).
36. Yan, H. *et al.* Programmable nanowire circuits for nanoprocessors. *Nature* **470,** 240–244 (2011).

Acknowledgements

This research was supported by the US Department of Energy, Office of Basic Energy Sciences, Division of Materials Sciences and Engineering (award no. DE-FG02-07ER46394), the National Science Foundation and the Knowledge Innovation Program of the Chinese Academy of Sciences (KJCX2-YW-M13). The authors thank Yushen Zhou and Sihong Wang for cleanroom work.

Author contributions

C.F.P. and Z.L.W. conceived and designed the project. C.F.P., L.D., G.Z., S.M.N., R.M.Y., Q.Y. and Y.L. designed, constructed and tested the apparatus. C.F.P., L.D. and Z.L.W. acquired the data and performed the analysis and simulation. Z.L.W. and C.F.P contributed to the preparation of the manuscript. All authors contributed to editing the manuscript.

Additional information

Supplementary information is available in the online version of the paper. Reprints and permissions information is available online at www.nature.com/reprints. Correspondence and requests for materials should be addressed to Z.L.W.

Competing financial interests

The authors declare no competing financial interests.